Bright squeezing from self-induced transparencies in dressed three-level atoms

M. K. Olsen

Department of Physics, University of Auckland, Private Bag 92019, Auckland, New Zealand

K. M. Gheri

Institut für Theoretische Physik, Universität Innsbruck, Technikerstrasse 25, A-6020 Innsbruck, Austria

D. F. Walls*

Joint Institute for Laboratory Astrophysics, University of Colorado, Boulder, Colorado 80309

We investigate two schemes for the efficient conversion of coherent input light into bright-squeezed output light. Both schemes utilize strong signal and weak probe fields, interacting with three-level ladder-configuration atoms inside optical cavities. The schemes differ in the resonance requirements of the cavities and produce noise suppression for quite different tuning regimes. Quantum-noise reduction is a consequence of the dressing of the atoms with two coherent fields. By tuning the probe light in the right fashion, spontaneous emission from the excited state can be made to counteract signal-light intensity fluctuations.

PACS number(s): 42.50.Lc, 42.50.Dv

I. INTRODUCTION

Despite the considerable recent advances in the generation of squeezed light [1], an efficient scheme that converts a strong coherent light beam into a beam with the same amplitude, but with reduced amplitude fluctuations, has not yet been discovered. Early squeezing experiments using two-level atoms were limited by the effects of spontaneous emission [2]. While the spontaneous emission could be reduced by tuning away from the atomic resonance, this also turns off the nonlinearity which generates the squeezing. Recent work which makes use of atomic coherence effects in coherently driven three-level atoms [3–5] offers the possibility of tailoring an atomic medium so that one can have a substantial nonlinear susceptibility with minimal absorption [6]. By means of a reduction of population in the excited state, the effect of spontaneous emission is thus reduced, giving an enhanced potential for the generation of squeezed light.

Recently, suggestions have been made for the utilization of spontaneous emission to reduce the amplitude fluctuations of a light field which drives and thereby saturates an atomic transition. It is well known that such a noise suppression effect is not present in two-level atomic systems. Coherence between the levels of the strongly driven transition and a third atomic energy level needs to be established. In recent papers, Gheri and Walls [7,8] have considered ensembles of three-level atoms in the Λ configuration interacting with a strong coherent signal on one transition and a weak probe on the other. They were able to demonstrate good amplitude squeezing on the signal output from the cavity.

In this paper we consider two systems, both of which utilize an ensemble of three-level atoms in the ladder (cascade) configuration, with a strong coherent signal on the upper transition and a weak probe on the lower one. In the first system, which we have named the *squeezer*, the optical cavity containing the atoms is tuned for resonance with the signal field only. The second, called the *ghost transition scheme*, requires that the cavity be resonant with both signal and probe fields. The use of ladder atoms should make the systems more easily experimentally realizable than the schemes of Gheri and Walls. The requirement for stabilization of the cavity to a single resonance should make the squeezer the easier to utilize of the two. The correlations that build up between the two light fields in the doubly resonant setup could, however, be exploited to further improve the squeezing; cf. Ref. [8]. Measurements performed on the probe output could be fed forward electronically and used to erase what is left in the signal output of the atomic noise that has been distributed to both light fields.

We will demonstrate below that the three-level ladder system will efficiently convert coherent input light into amplitude squeezed output light for both experimental setups. While it might appear that the ladder atoms would be more susceptible to the effects of spontaneous emission than the Λ atoms, our calculations show that the effect is slight. Since the semiclassical portions of the calculations are almost identical for the two schemes, the first part of this paper will apply to both schemes. The particular fluctuation analyses for each scheme will be presented separately in self-contained sections.

II. MOTIVATION

Consider a closed two-level atom driven by a coherent light field whose Rabi frequency Ω greatly exceeds the

---

*Permanent address: Department of Physics, University of Auckland, Private Bag 92019, Auckland, New Zealand.

natural linewidth γ of the excited state. The light field will saturate the system and both levels will be almost equally populated. At first glance one might expect that the loss incurred by the light field due to spontaneous emission from the excited state could constitute a potential mechanism for suppressing the intensity fluctuations of the light provided the interaction takes place inside a cavity. Any increase in intracavity intensity would lead to more population in the excited state and thus increase the loss due to a larger number of spontaneously emitted photons.

However, this is not the case. The rate γ_a at which photons are absorbed from the light field is not solely determined by the population in the excited state σ_{ee}, but is modified by the field such that

$$\gamma_a \propto \frac{\gamma^2}{|\Omega|^2}\sigma_{ee}. \qquad (1)$$

Clearly, a stronger light field not only increases the excited state population but also makes an incoherent process such as spontaneous decay less likely. This phenomenon is well known and is usually referred to as *bleaching*.

However, the same need not hold for more complicated level configurations. What we would like to find is a system consisting of a strongly driven atomic transition that is *open* and in which fluctuations in the intensity of the driving light will result in a change of the atoms' absorptive response, thereby counteracting the fluctuations. By open we mean that one of the two levels is connected to a further level by means of a bidirectional coupling so as to ensure a nonvanishing level population. Note that it is essential for the field to saturate the transition so as to minimize the loss experienced by the mean amplitude of the field.

It is quite clear that this coupling cannot be of an incoherent nature as this would change the level populations but not the nature of the response of the atoms. It would thus appear that a *coherent* coupling to a third level is required. If we operate in a tuning limit where the coherent coupling has a significant impact on the system dynamics strong coherences between all levels build up; cf. Sec. IV. In this case we can no longer consider the levels as being independent of each other. As we have in fact changed the system characteristics by involving a third level in the response of the atoms to the strong light field, we may hope to have achieved a qualitative change in the atoms' response.

Applying a second coherent field would allow us to tailor the atomic response by altering the frequency and intensity of this field. In the following we will analyze two methods whereby this idea can be realized with a medium of three-level ladder-configuration atoms inside an optical cavity.

III. BASIC EQUATIONS

The general system under consideration is an ensemble of three-level atoms in the ladder (cascade) configuration,

as shown in Fig. 1, contained in an optical resonator. These atoms interact with a strong coherent signal (described by boson operators a_2 and $a_2^\dagger$) and a weak probe field (described by a_1 and $a_1^\dagger$). The Rabi frequencies of the signal and probe satisfy $|\Omega_s| \gg |\Omega_p|$. The signal field is assumed to be at resonance with the upper transition, although this is not a prerequisite, and the probe is detuned by Δ from the lower transition. The spontaneous decay rates and detuning are as shown in Fig. 1.

In our analysis we begin by adapting the equations of motion given by Poizat, Collett, and Walls in [9]. Neglecting the position dependence gives us the following system of equations:

$$\frac{da_j}{dt} = -\kappa_j(1 + i\phi_j)a_j + g_j\sigma_{jj+1} - \sqrt{2\kappa_j}a_j^{\text{in}}, \qquad (2a)$$

$$\frac{d\sigma_{11}}{dt} = 2\gamma_1\sigma_{22} + g_1(\sigma_{21}a_1 + a_1^\dagger\sigma_{12})$$
$$+ \sqrt{2\gamma_1}\,(\sigma_{21}\beta_1^{\text{in}} + \beta_1^{\text{in}\dagger}\sigma_{12}), \qquad (2b)$$

$$\frac{d\sigma_{33}}{dt} = -2\gamma_2\sigma_{33} - g_2(\sigma_{32}a_2 + a_2^\dagger\sigma_{23})$$
$$- \sqrt{2\gamma_2}\,(\sigma_{32}\beta_2^{\text{in}} + \beta_2^{\text{in}\dagger}\sigma_{23}), \qquad (2c)$$

$$\frac{d\sigma_{12}}{dt} = -(\gamma_1 + i\Delta)\sigma_{12} + g_1a_1(\sigma_{22} - \sigma_{11}) + g_2a_2^\dagger\sigma_{13}$$
$$+ \sqrt{2\gamma_1}(\sigma_{22} - \sigma_{11})\beta_1^{\text{in}} + \sqrt{2\gamma_2}\,\beta_2^{\text{in}\dagger}\sigma_{13}, \qquad (2d)$$

$$\frac{d\sigma_{23}}{dt} = -(\gamma_1 + \gamma_2)\sigma_{23} - g_1a_1^\dagger\sigma_{13} + g_2a_2(\sigma_{33} - \sigma_{22})$$
$$- \sqrt{2\gamma_1}\beta_1^{\text{in}\dagger}\sigma_{13} + \sqrt{2\gamma_2}(\sigma_{33} - \sigma_{22})\beta_2^{\text{in}}, \qquad (2e)$$

$$\frac{d\sigma_{13}}{dt} = -(\gamma_2 + i\Delta)\sigma_{13} + g_1a_1\sigma_{23} - g_2a_2\sigma_{12}$$
$$+ \sqrt{2\gamma_1}\,\sigma_{23}\beta_1^{\text{in}} - \sqrt{2\gamma_2}\,\sigma_{12}\beta_2^{\text{in}}, \qquad (2f)$$

along with the obvious equations for the three conjugate variables. Note that g_j, assumed to be real, is the coupling constant for mode j and κ_j are the respective cavity decay rates. Also note the assumed closure relation for the atomic population operators: $\Sigma_{j=1}^3\sigma_{jj} = 1$. In the
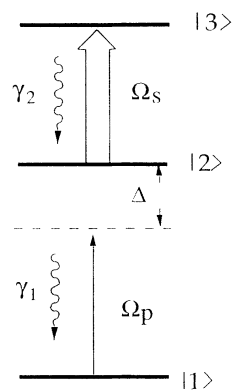

FIG. 1. Energy level diagram of a three-level atom in the ladder configuration driven by two coherent fields with Rabi frequencies Ω_s and Ω_p. The strong signal field is tuned to resonance while the probe is detuned by Δ. The spontaneous decay rates are denoted by $2\gamma_1$ and $2\gamma_2$, respectively.

setup under consideration, ϕ_j is the mistuning (in units of κ_j) between the input and cavity fields, chosen such that the cavity mistuning due to the presence of the atoms is compensated for. This means that the input fields are resonant with the respective cavities at all times. The atomic operators have been defined

$$\sigma_{ij} = \frac{1}{N} \sum_{\mu=1}^{N} \sigma_{ij}^{\mu}, \tag{3}$$

where σ_{ij}^{μ} denotes the coherence operator between levels i and j of the μth atom. These operators obey the multiplication rule $\sigma_{ij}\sigma_{kl} = \sigma_{il}\delta_{jk}/N$. The β_j^{in} are stochastic atomic noise operators. For the particular case of the squeezer, we do not need to consider probe fluctuations, so we can make the simplification of replacing $g_1 a_1$ by its semiclassical equivalent Ω_p. For use below, we also define the cooperativity for each mode [10], $C_j = g_j^2 N/\kappa_j \gamma_j$, a quantity which characterizes the strength of the collective interactions of the N atoms with the respective cavity mode.

Going to the quantum white noise limit, it is immediately apparent that this system can be treated as an Ornstein-Uhlenbeck process in the atomic variables. This is equivalent to a system description via a master equation, which, while containing less information than Langevin equations, is more convenient for our system. There is no difference in the assumed vacuum state of the baths. Since we are interested in the atomic variables, we use Eqs. (2b)–(2f) to give the quantum stochastic differential equation

$$d\vec{\sigma} = -(\mathbf{M}_0 \vec{\sigma} - \vec{a})dt + d\vec{\beta}(t), \tag{4}$$

in which the matrix $\mathbf{M}_0$ gives the time evolution of the atomic variables for given values of the fields while $d\vec{\beta}(t)$ is treated as a vector of quantum Itô noise increments.

The above system of nonlinear operator equations can be readily solved via linearization [11]. Setting the noise increments to zero and treating the system operators as c numbers allows us to determine the semiclassical deterministic aspects of the interaction. This entails setting $\Omega_j = g_j a_j$. Having performed a system size expansion [12] in terms of N, the number of atoms, system fluctuations will be described by correction terms of the order $1/\sqrt{N}$. We find for the deterministic equation

$$\frac{d\vec{\sigma}}{dt} = -\mathbf{M}_0 \vec{\sigma} + \vec{a}, \tag{5}$$

which, for the steady-state, obviously gives

$$\vec{\sigma} = \mathbf{M}_0^{-1} \vec{a}. \tag{6}$$

IV. SEMICLASSICAL SOLUTIONS

Although exact analytical expressions can be obtained for the density matrix elements, they are rather unwieldy. We are interested in the regime in which $\Delta \approx |\Omega_s|$ and $|\Omega_s| \gg |\Omega_p|$ and fortunately find that this regime is an-

alytically accessible. Thus upon replacing Δ by $\Delta_0 + \nu$ and Δ_0^2 by $|\Omega_s|^2$ (note that $I_s = |\Omega_s|^2$ and $I_p = |\Omega_p|^2$) and carrying out an asymptotic series expansion in the small parameter $1/|\Omega_s|$, we obtain much simpler expressions. The large coherences established in the atomic system create finite contributions for all σ_{ij}, even in lowest order. In particular, after also setting $\Gamma = \gamma_1 + \gamma_2$, we find

$$\sigma_{13} = -\frac{\Omega_s \Omega_p \gamma_1}{|\Omega_s| D_0} (2\nu + i\Gamma), \tag{7a}$$

$$\sigma_{32} = -\frac{\Omega_s^*}{D_0} \left(\frac{\Gamma \gamma_2 I_p}{I_s} + i \frac{\gamma_1 I_p}{|\Omega_s|} \right), \tag{7b}$$

$$\sigma_{12} = -\frac{\Omega_p \gamma_1}{D_0} (\Gamma - 2i\nu), \tag{7c}$$

$$\sigma_{11} = \frac{(\Gamma^2 + 4\nu^2)\gamma_1 + I_p(\Gamma + \gamma_1)}{D_0}, \tag{7d}$$

$$\sigma_{33} = \frac{I_p \Gamma}{D_0}, \tag{7e}$$

$$\sigma_{33} - \sigma_{22} = -\frac{2I_p \nu \gamma_1}{D_0 |\Omega_s|}, \tag{7f}$$

with all expressions having the common denominator

$$D_0 = I_p(3\Gamma + \gamma_1) + \gamma_1(\Gamma^2 + 4\nu^2). \tag{8}$$

The above are remarkably similar to the expressions obtained by Gheri and Walls [7] for the Λ system in the same regime. It seems that, at least in lowest order, the ladder system is almost completely equivalent to a Λ system with the signal transition rotated about the upper level. The one immediate difference is that we now require a negative detuning to obtain inversion on the signal transition (7f). This can be understood as follows: clearly, Λ and ladder atoms are equivalent as far as purely coherent processes are concerned. In our tuning limit the coherent interactions dominate the semiclassical behavior. Thus in going from the Λ to the ladder scheme (as far as the population inversion is concerned) it is sufficient to interchange the labeling of the ground and excited states.

V. THE SQUEEZER MODEL

A. Mesoscopic quantum fluctuation analysis

We will now proceed to analyze the quantum statistical properties of the system. Assuming the fluctuations to be small, we may use a linearized fluctuation analysis. Consequently, the quantum stochastic properties of the field depend on both the linear atomic response to the field and on atomic noise terms describing spontaneous emission. This can be most concisely formulated in the frequency domain, in terms of susceptibility coefficients χ_{kl}, where k and l represent the signal field quadratures. This establishes a linear relationship between fluctuations in the atomic polarizations and the light field [13,14]. Since it is convenient to use quadrature operators, we define

$$X_s = \frac{\alpha^*}{|\alpha|}\delta a + \frac{\alpha}{|\alpha|}\delta a^\dagger, \qquad (9a)$$

$$Y_s = -i\left(\frac{\alpha^*}{|\alpha|}\delta a - \frac{\alpha}{|\alpha|}\delta a^\dagger\right). \qquad (9b)$$

The annihilation and creation operators for the fluctuations in the signal-light field are denoted by δa and $\delta a^\dagger$ and α is the macroscopic mean complex amplitude of the signal mode.

Arranging the signal quadrature operators (with the reference phase given by the cavity field and the subscript denoting the squeezer model) in a column vector $\vec{X}_{sq}(t) = (X_s(t), Y_s(t))^T$, we can write the time evolution of the intracavity signal fluctuations in the general form

$$d\vec{X}_{sq}(t) = d\mathbf{L}_{f,sq}(t)\vec{X}_{sq}(t) + \vec{R}_{sq}(t)dt, \qquad (10)$$

where $\vec{R}_{sq}(t)$ denotes the atomic contribution to the signal fluctuations and the Liouvillian superoperator $d\mathbf{L}_{f,sq}(t)$ describes the evolution of the mode in an empty cavity [15].

In the frequency domain $\vec{R}_{sq}(\omega)$ can be expressed as a linear superposition of the driving field fluctuation terms and the statistically independent noise terms. We find the simple relation

$$\vec{R}_{sq}(\omega) = \boldsymbol{\chi}_{sq}(\omega)\vec{X}_{sq}(\omega) + \vec{\beta}_{sq}(\omega), \qquad (11)$$

where the atomic noise quadrature operators are arranged in the vector $\vec{\beta}_{sq}(\omega)$, which allows us to define the atomic noise correlation matrix for the total system $\mathbf{G}(\omega)\delta(\omega + \nu) = \langle\vec{\beta}(\omega)\vec{\beta}^T(\nu)\rangle$.

Although the relationships given in this section so far will hold for arbitrary frequency, from now on we will take advantage of the formal similarity between a zero-frequency fluctuation analysis and an adiabatic analysis. A zero-frequency analysis applies only to slow field fluctuations, which the atoms will follow adiabatically.

To develop the zero-frequency susceptibility coefficients, we begin with the actual microscopic operator-valued coefficient $\chi_s^{mic}(a, a^\dagger)$. We can define a nonlinear semiclassical susceptibility coefficient $\chi_s(\alpha, \alpha^*)$ by the relationship

$$\chi_s = C_s\gamma_2\frac{\langle\sigma_{23}\rangle}{\Omega_s}. \qquad (12)$$

Linearizing the mode operators around their expectation values so that $a = \alpha + \delta a$, we can expand χ_s^{mic} in terms of χ_s:

$$\chi_s^{mic}(a, a^\dagger)a = \chi_s(\alpha, \alpha^*)\alpha + \chi_s(\alpha, \alpha^*)\delta a$$
$$+ \alpha\frac{\partial\chi_s}{\partial\alpha}\delta a + \alpha\frac{\partial\chi_s}{\partial\alpha^*}\delta a^\dagger + O(2). \qquad (13)$$

Noting that

$$\frac{\partial\chi_s}{\partial\alpha} = \frac{\partial\chi_s}{\partial I_s}\frac{\partial I_s}{\partial\alpha} \qquad (14)$$

and

$$\frac{\partial I_s}{\partial\alpha} = \alpha^*, \qquad (15)$$

we see that

$$\alpha\frac{\partial\chi_s}{\partial\alpha}\delta a = I_s\frac{\partial\chi_s}{\partial I_s}\delta a. \qquad (16)$$

Using the fluctuation equation of motion

$$\kappa^{-1}\partial_t\delta a = -(1 + i\phi)\delta a + \chi_s^{mic}a$$
$$- \chi_s\alpha - \sqrt{2/\kappa}\delta a^{in} + \eta_{at}, \qquad (17)$$

where η_{at} represents atomic noise, and combining δa and $\delta a^\dagger$ in the quadrature operators defined above, we arrive at the equation

$$\kappa^{-1}\partial_t X_s = [\mathrm{Re}(\chi_s) - 1]X_s + 2I_s\frac{\partial\mathrm{Re}(\chi_s)}{\partial I_s}X_s$$
$$+ [\phi - \mathrm{Im}(\chi_s)]Y_s - \sqrt{2/\kappa}X_s^{in} + X_s^a, \qquad (18)$$

where X_s^a denotes the atomic noise operator perturbing the cavity amplitude. Note that all quadrature operators are defined with respect to the phase of the mean cavity field. Since in this particular case we are interested in absorption of the signal, this allows us to define

$$\chi_{XX} = -1 + \mathrm{Re}(\chi_s) + 2I_s\partial_{I_s}\mathrm{Re}(\chi_s), \qquad (19)$$

in which $\mathrm{Re}(\chi_s)$ becomes the linear absorption coefficient and $2I_s\partial_{I_s}\mathrm{Re}(\chi_s)$ becomes the nonlinear absorption coefficient. Proceeding in a similar manner, we can define

$$\chi_{YY} = -1 + \mathrm{Re}(\chi_s), \qquad (20a)$$

$$\chi_{XY} = \phi - \mathrm{Im}(\chi_s), \qquad (20b)$$

$$\chi_{YX} = -\phi + \mathrm{Im}(\chi_s) + 2I_s\partial_{I_s}\mathrm{Im}(\chi_s). \qquad (20c)$$

Note that, as already stated, we assume that ϕ is chosen such that χ_{XY} vanishes for zero frequency. This is tantamount to keeping the cavity resonant with the input field in the presence of an intracavity medium. Again to lowest order, we find [16]

$$\chi_{XX} = -1 - \frac{C_s\Gamma\gamma_2^2 I_p}{|\Omega_s|D_0}\left(\frac{1}{|\Omega_s|} + \frac{8\nu\gamma_1}{D_0}\right), \qquad (21a)$$

$$\chi_{YY} = -1 - \frac{C_s I_p\Gamma\gamma_2^2}{I_s D_0}, \qquad (21b)$$

$$\chi_{YX} = \frac{8C_s I_p\gamma_1^2\gamma_2\nu}{D_0^2}. \qquad (21c)$$

Following the usual procedure for Ornstein-Uhlenbeck processes [11], we derive, for the excess atomic noise in the intracavity signal (i.e., the variances and covariances of the atomic noise operators X_s^a and Y_s^a),

$$\mathbf{N}_{cav}^{ex}|_{\omega=0} = \mathbf{Q}\mathbf{M}_0^{-1}\mathbf{G}(\mathbf{M}_0^{-1})^T\mathbf{Q}^T, \qquad (22)$$

where $\mathbf{Q}$ is the amplitude and phase quadrature generating matrix $\sqrt{C_s\gamma_2/\kappa}\,\mathbf{Q}_0\mathbf{P}_{ij}$, with

$$\mathbf{Q}_0 = \begin{bmatrix} 1 & 1 \\ -i & i \end{bmatrix}, \qquad (23)$$

and $\mathbf{P}_{ij}$ is a projector which selects the appropriate rows i and j of $\mathbf{M}_0^{-1}$. For later use, we define

$$\mathbf{N}_{\mathrm{cav}}^{\mathrm{ex}}|_{\omega=0} = \kappa^{-1} \begin{bmatrix} u & r+is \\ r-is & v \end{bmatrix}. \qquad (24)$$

Although an analytical expression can be obtained for the atomic noise, it is rather complicated and not very illuminating, in contrast to the Λ system, where a reasonably simple expression can be derived. The obvious explanation for this is that spontaneous emission processes can play a greater role on the signal transition of the ladder system, thereby complicating the analysis. Therefore relationship (22) is mostly useful for numerical simulations.

In order to predict the degree of amplitude squeezing in the output signal, we must now calculate $\mathrm{Var}(X_s^{\mathrm{out}})$. Using the standard input-output relationship

$$X_s^{\mathrm{out}} = X_s^{\mathrm{in}} + \sqrt{2\kappa}\, X_s \qquad (25)$$

and the zero-frequency equation of motion

$$\vec{0} = \chi_{\mathrm{sq}}(0)\vec{X}_{\mathrm{sq}} + \vec{X}_{\mathrm{sq}}^a - \sqrt{2/\kappa}\,\vec{X}_{\mathrm{sq}}^{\mathrm{in}}, \qquad (26)$$

where $\chi_{\mathrm{sq}}(0)$ denotes the matrix of zero-frequency susceptibility coefficients of Eqs. (19)-(20c), we find, for the output signal amplitude variance,
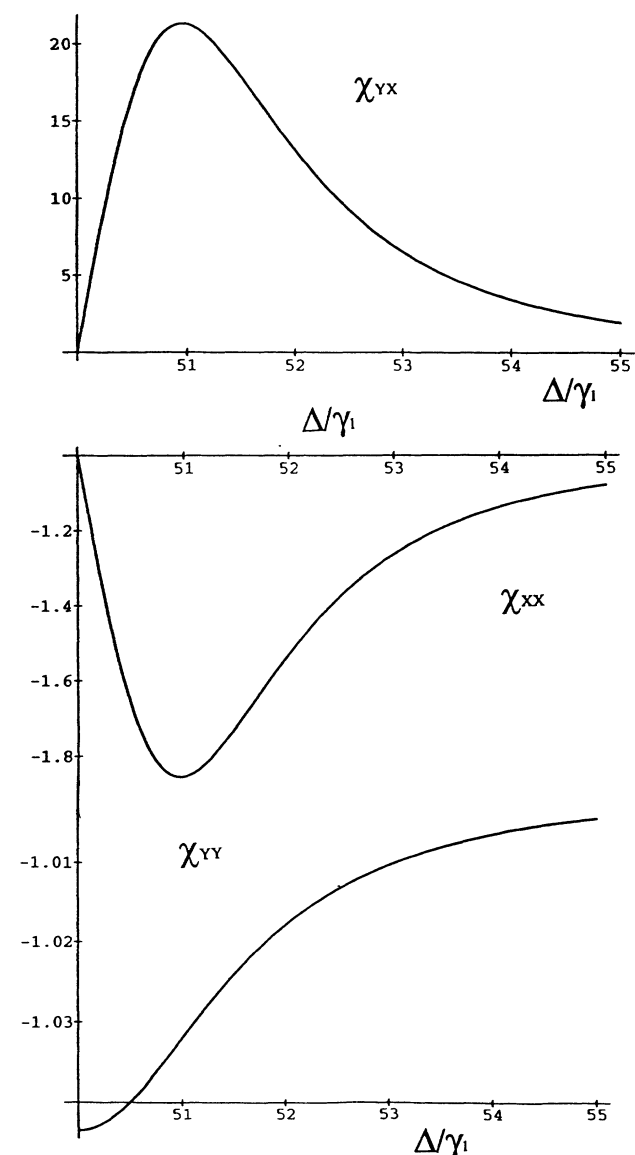
$$\mathrm{Var}(X_s^{\mathrm{out}})|_{\omega=0} = \frac{\xi(\xi + 4\chi_{YY}) + \chi_{YY}^2(4+2u) + \chi_{XY}^2(4+2v) - 4r\chi_{YY}\chi_{XY}}{\xi^2}, \qquad (27)$$

where $\xi = \chi_{XX}\chi_{YY} - \chi_{XY}\chi_{YX}$. We have plotted the zero-frequency χ coefficients as functions of detuning, from which it can be seen that the denominator in the above expression is largest around one linewidth from the Rabi-split level; cf. Fig. 2. For the parameters used, this is the region of best squeezing. In this regime of optimum squeezing, we find that almost all of $\mathrm{Var}(X_s^{\mathrm{out}})$ is due to the intracavity atomic noise contribution and almost none from the input field. During numerical trials we found that a large degree of squeezing in the amplitude quadrature was available over a broad parameter range.

However, since the fluctuation reduction is due to spontaneous emission processes, a large amount of excess noise is injected into the phase quadrature. The output signal is no longer in a minimum uncertainty state, as shown in our numerical computations, where, for example, an amplitude quadrature variance of approximately 0.1 would be accompanied by a phase quadrature variance of the order of 1000. The product of the amplitude and phase variances thus exceeds the Heisenberg limit by a rather large factor.

We were able to obtain a lowest order analytical approximation to the signal amplitude output variance which compares well with the numerical trials, showing that the series expansion is valid for this system. The graphic results presented have been plotted for the zero-frequency component of the signal spectrum. Figure 3 shows the results for the following set of parameters: C_s(cooperativity)$= 600$, $\gamma_1 = \gamma_2 = 1$, $\kappa_s = 0.1$, $|\Omega_p| = 1$, and $|\Omega_s| = 50$. It can readily be seen that $\langle(X_s^{\mathrm{out}}X_s^{\mathrm{in}})\rangle^2$ drops very close to zero and almost all the output fluctuations are due to intracavity atomic noise. The attainment of good squeezing depends significantly on achieving the optimum combination of cooperativity, signal amplitude, and detuning. For a given set of parameters, it seems that the expected squeezing from the ladder system is very slightly inferior to that predicted by Gheri and Walls [7] for the Λ system. This is to be expected since spontaneous emission is a more pronounced feature of the ladder system.

We have also considered degradation of the squeezing from atomic losses to a fourth level and from dephasing of the signal transition via atomic collisions. The inclusion

FIG. 2. Lowest order analytical approximations for the three nonzero χ coefficients for the squeezer. These are the values used in the analytical approximation plotted for the signal output variance in Fig. 3, and are plotted for the same parameters.
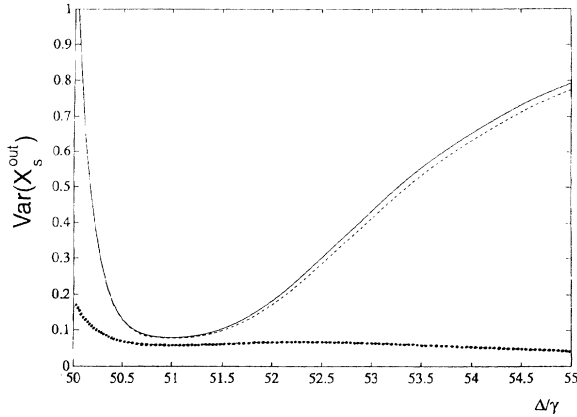
FIG. 3. Signal output variance for the squeezer, showing considerable squeezing at zero frequency for the following parameters: $C_s = 600, \gamma_1 = \gamma_2 = 1, |\Omega_p| = 1, |\Omega_s| = 50$, and $\kappa_s = 0.1$. The dashed line is the lowest order analytical approximation and the dotted line is $\langle (X_s^{out} X_s^{in}) \rangle^2$ for the same parameters.

of physical values which we consider realistic for these effects still leaves significant amplitude squeezing. Figure 4 shows a set of results with these effects included. Atomic number fluctuations would not be expected to have a significant effect as long as they happen on a far longer time scale than the spontaneous emission processes on which the squeezing depends.

B. Discussion

We have shown that an ensemble of driven ladder-configuration atoms in a singly resonant optical cavity
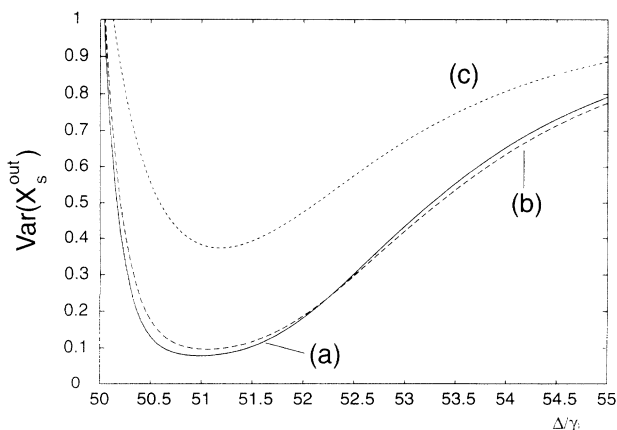

FIG. 4. Effects for the squeezer due to dephasing and atomic losses for the same parameters as Fig. 3. (a) The zero-frequency signal output variance as above. (b) The effect expected from a dephasing constant of $0.5\gamma_1$. We suspect that dephasing can reduce the variance for some detunings via a dynamic noise suppression effect. (c) The variance with atomic losses to a level below the ground state of the system taken into account. The atoms also cycle to and from this level at the same rate of $0.1\gamma_1$.

can produce a highly squeezed output signal without significant degradation of the input. The effect requires that a weak probe field on the lower transition be tuned close to one of the split Rabi states generated by a strong signal field on the upper transition. A fluctuation in the input field into the cavity may cause an increase in the signal amplitude, thus increasing the Rabi splitting of the intermediate level. This moves the probe field closer to resonance with the lower transition, hence increasing the rate of population transfer from the ground state to the intermediate level. The higher proportion of atoms in the intermediate state can now absorb more photons from the signal, hence damping out the amplitude fluctuation. A shortage of photons in the signal mode likewise leads to a proportional reduction in the population in the intermediate level and thus a lesser rate of absorption of signal photons. The photon number fluctuations are dramatically reduced by this process, while the dependence on spontaneous emission greatly increases the phase fluctuations.

The overall effect is that the strength of the signal input causes a self-induced transparency in the upper atomic transition, enabling an almost lossless transmission of the signal. However, the increase in phase fluctuations means that the transmitted signal is now far from being in a minimum uncertainty state.

VI. THE GHOST TRANSITION SCHEME

If we allow both the signal and probe fields to be resonant within cavities, strong correlations build up between the signal and probe phase quadrature fluctuations and two photon coherences now play a dominant role. When the probe field is tuned inside the signal-split Autler-Townes doublet, a ghost transition (emptying of the lower signal level via optical pumping) is created. This has previously been exploited for a quantum nondemolition (QND) measurement scheme [10]. A successful experimental demonstration of a QND measurement using the ghost transition scheme has been accomplished by Poizat and Grangier [17].

In this section we will investigate the potential of the ghost transition scheme for the reduction of output signal amplitude fluctuations. An analysis of a similar scheme, using three-level Λ atoms, by Gheri and Walls [8] has predicted significant quantum-noise reduction. Since the QND experiments of Poizat and Grangier were performed on three-level ladder atoms, we shall investigate the potential for squeezing in this system. The effect of having the probe resonant with the cavity is that any probe fluctuations can act back on the signal, building up correlations between the two modes. This can either reduce or increase the signal amplitude fluctuations, depending on the detuning of the probe from the lower atomic transition. The mechanism for the squeezing is the correlation which builds up between the two modes. The fact that this is completely different from the mechanism at work in the squeezer is shown by the system becoming unstable for the tuning configuration which gives good noise reduction in the squeezer.

A. Mesoscopic quantum fluctuation analysis

The fluctuation analysis for the ghost transition scheme proceeds in a similar manner to that carried out above for the squeezer model, with the additional complication that we must now also consider fluctuations in the probe field. This is because the doubly resonant cavity allows cross correlations between the two intracavity fields to develop. Arranging all quadrature operators (with the reference phases given by the respective input fields) in a column vector $\vec{X}_{\rm gh}(t) = (X_s(t), Y_s(t), X_p(t), Y_p(t))^T$, with the subscript having the obvious meaning, we can again write the time evolution of the intracavity mode fluctuations in the general form

$$d\vec{X}_{\rm gh}(t) = d\mathbf{L}_{f,\rm gh}(t)\vec{X}_{\rm gh}(t) + \vec{R}_{\rm gh}(t)dt, \qquad (28)$$

where $\vec{R}_{\rm gh}(t)$ and $d\mathbf{L}_{f,\rm gh}(t)$ have analogous meanings to those used in the squeezer analysis above.

The zero-frequency susceptibility coefficients are again derived from the semiclassical solutions given above in Eq. (7), performing Taylor expansions of the susceptibility coefficients in terms of the mode operators. In particular, noting that the cooperativity C_j describes the strength of the coupling between cavity mode j and the atomic medium, and defining

$$\chi_s = \gamma_2 C_s \frac{\langle \sigma_{23} \rangle}{\Omega_s}, \quad \chi_p = \gamma_1 C_p \frac{\langle \sigma_{12} \rangle}{\Omega_p}, \qquad (29a)$$

$$\chi_{ss} = -1 + {\rm Re}(\chi_s) + 2I_s \partial_{I_s} {\rm Re}(\chi_s), \qquad (29b)$$

$$\chi_{pp} = -1 + {\rm Re}(\chi_p) + 2I_p \partial_{I_p} {\rm Re}(\chi_p), \qquad (29c)$$

$$\chi_{sp} = 2\sqrt{C_p \gamma_1 \kappa_p / C_s \gamma_2 \kappa_s}|\Omega_s||\Omega_p|\partial_{I_p}{\rm Re}(\chi_s), \qquad (29d)$$

$$\chi_{ps} = 2\sqrt{C_s \gamma_2 \kappa_s / C_p \gamma_1 \kappa_p}|\Omega_s||\Omega_p|\partial_{I_s}{\rm Re}(\chi_p), \qquad (29e)$$

we find, again to lowest order in $1/|\Omega_s|$ [cf. Eq. (21)],

$$\chi_{ss} = -1 - \frac{C_s \Gamma \gamma_2^2 I_p}{D_0 |\Omega_s|}\left[\frac{1}{|\Omega_s|} + \frac{8\nu\gamma_1}{D_0}\right], \qquad (30a)$$

$$\chi_{pp} = -1 + C_p \Gamma \gamma_1^2[I_p(3\Gamma + \gamma_1) - \gamma_1(\Gamma^2 + 4\nu^2)]/D_0^2, \qquad (30b)$$

$$\chi_{sp} = -2\sqrt{C_s C_p \gamma_1^3 \gamma_2^3 I_p \kappa_p / I_s \kappa_s}\,\Gamma(\Gamma^2 + 4\nu^2)/D_0^2, \qquad (30c)$$

$$\chi_{ps} = -8\Gamma\nu\sqrt{C_s C_p \gamma_1^5 \gamma_2 I_p \kappa_s / \kappa_p}/D_0^2. \qquad (30d)$$

In Fig. 5 we have plotted the coefficients above as functions of ν to develop a feeling for their relative size. Note that χ_{pp} and χ_{ps} are much larger than their respective counterparts for the signal amplitude.

To calculate ${\rm Var}(X_s^{\rm out})$, the quantity of interest, we define $n_j = {\rm Var}(X_j^a)$ and $n_c = \frac{1}{2}\langle X_p^a X_s^a + X_s^a X_p^a \rangle - \langle X_p^a \rangle \langle X_s^a \rangle$, where X_j^a is the intracavity atomic noise in the amplitude quadrature of the jth atomic transition. By using the standard input-output relationship and the zero-frequency equation of motion

$$\vec{0} = \chi_{\rm gh}(0)\vec{X}_{\rm gh} + \vec{X}_{\rm gh}^a - \sqrt{2/\kappa}\,\vec{X}_{\rm gh}^{\rm in}, \qquad (31)$$

where $\chi_{\rm gh}(0)$ denotes the matrix of susceptibility coefficients and $\sqrt{2/\kappa}$ is a diagonal matrix, we arrive at the formula for the zero-frequency variance in the output signal amplitude quadrature

$${\rm Var}(X_s^{\rm out})|_{\omega=0} = \frac{(\lambda + 2\chi_{pp})^2 + 2\kappa_s[n_s\chi_{pp}^2 - 2n_c\chi_{sp}\chi_{pp} + \chi_{sp}^2(2/\kappa_p + n_p)]}{\lambda^2}, \qquad (32)$$
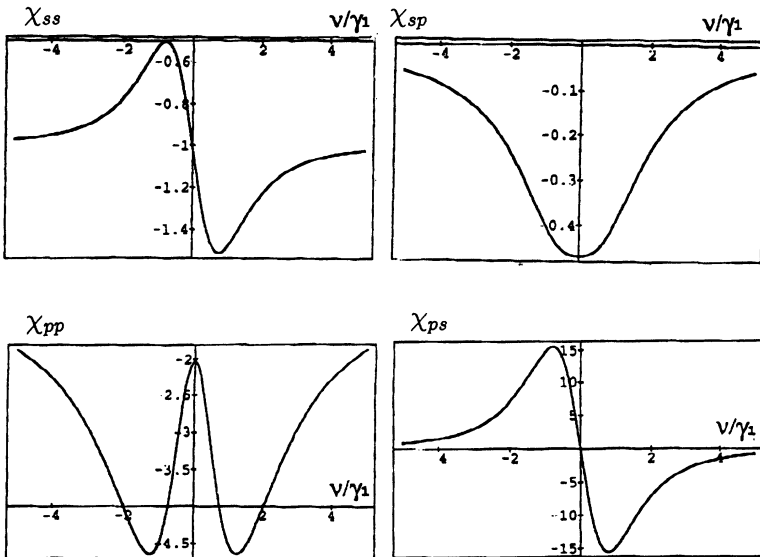

FIG. 5. Lowest order analytical approximations to the amplitude-amplitude susceptibilities for the ghost transition scheme, using the following parameters, with all frequencies in units of γ_1: $\Omega_s = 75$, $\Omega_p = 0.7$, $C_s = 600$, $C_p = 50$, $\kappa_s = \kappa_p = 0.5$, and $\gamma_2 = 1$.

where $\lambda = \chi_{ss}\chi_{pp} - \chi_{ps}\chi_{sp}$.

The amplitude-amplitude atomic noise correlation terms below are calculated as for the squeezer, again to lowest order in $1/|\Omega_s|$. In order to assist with ease of computation and give analytical results in a sensibly concise form, we set $\gamma_1 = \gamma_2 = \frac{1}{2}\Gamma$ before proceeding [18]. This allows us to find the explicit expressions

$$n_s = \frac{2C_s\Gamma^2 I_p[3(\Gamma^2 + 4\nu^2)^2 + I_p(14\Gamma^2 + 59I_p + 120\nu^2)]}{\kappa_s I_s D_1^3},$$

(33a)

$$n_p = \frac{2C_p\Gamma^2[(\Gamma^2 + 4\nu^2)^2 + I_p(45I_p + 56\nu^2 - 2\Gamma^2)]}{\kappa_p D_1^3},$$

(33b)

$$n_c = \frac{\Gamma^2\sqrt{C_s C_p I_p}}{D_1^3\sqrt{\kappa_p\kappa_s I_s}}[(\Gamma^2 + 4\nu^2)^2 + I_p(3I_p^2 - 8\Gamma^2 + 32\nu^2)]$$

(33c)

with the common denominator

$$D_1 = \Gamma^2 + 7I_p + 4\nu^2.$$

(34)

B. Numerical trials

Although the analytical expression for $\mathrm{Var}(X_s^{\mathrm{out}})$ derived via the above procedure is too unwieldy to reproduce here, it can be plotted for comparison with numerical trials. Figure 6 shows the result of one such trial. It can immediately be seen that the lowest order terms from the asymptotic expansion agree well with the overall form of the full numerical result in the parameter regime chosen, although there is some discrepancy if we consider the difference from ideal squeezing. We would expect that the deviation here would be less than any experimental uncertainties which would be introduced in a practical realization of the scheme. There seems to be no reason why the degree of agreement would not hold over a wide
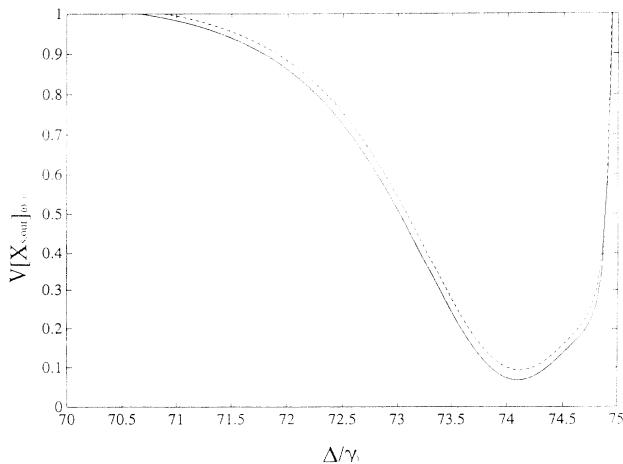

FIG. 6. Zero-frequency variance in the output signal for the ghost transition scheme. The solid line is the full numerical solution while the dashed line is the lowest order analytical approximation, both for the same parameters as in Fig. 5.

range of field intensities, so long as $|\Omega_s| \gg |\Omega_p|, \gamma_1, \nu$ so that the expansion in terms of $1/|\Omega_s|$ remains valid.

It can be seen that the range of detunings over which good zero-frequency squeezing is available is smaller than for the squeezer model, and the sign of the detuning has changed. This is because the probe is now tuned to the inside of the Autler-Townes doublet. The squeezing is not the absolute maximum theoretically achievable, but can be improved by further increasing C_s and $|\Omega_s|$.

C. The physical mechanism

The unusual tuning limit of a weak probe being far from resonance with the $|1\rangle$ to $|2\rangle$ transition indicates that two-photon processes are important in the ghost transition scheme. Formally this is manifested by the elements σ_{12} and σ_{23} of the atomic polarization containing significant contributions from the two-photon coherence σ_{13}. By taking the semiclassical steady-state solutions of the equations of motion [cf. Eq. (7)] we can readily show

$$\sigma_{12} = \frac{\Omega_p}{\gamma_1 + i\Delta}\left(\sigma_{22} - \sigma_{11} + \frac{\Omega_s^*\Omega_p^*}{|\Omega_p|^2}\sigma_{13}\right),$$

(35a)

$$\sigma_{23} = \frac{\Omega_s}{\gamma_1 + \gamma_2}\left(\sigma_{33} - \sigma_{22} - \frac{\Omega_p^*\Omega_s^*}{|\Omega_s|^2}\sigma_{13}\right).$$

(35b)

Comparison of the different sizes expected from the individual terms, noting that $\sigma_{11} \gg \sigma_{22}$ and $\sigma_{22} \approx \sigma_{33}$, demonstrates our contention of the relative importance of two-photon processes. Assigning to the various parameters the values used in Fig. 6 and taking $\nu = -1$, the approximate detuning of maximum squeezing, we find

$$\sigma_{22} - \sigma_{11} \approx -0.743,$$

(36a)

$$\sigma_{33} - \sigma_{22} \approx 0.0011,$$

(36b)

$$\mathrm{Im}\left(\frac{\Omega_p^*\Omega_s^*}{|\Omega_p|^2}\sigma_{13}\right) \approx -13.12,$$

(36c)

$$\mathrm{Re}\left(\frac{\Omega_s^*\Omega_p^*}{|\Omega_s|^2}\sigma_{13}\right) \approx 0.0011.$$

(36d)

The relative sizes of these terms mean that stimulated absorptive or emissive events on one transition will always have an effect on the field dressing the other transition.

The loss of a signal photon can provoke the emission of a probe photon induced by the two-photon coherence σ_{13}. The decrease in the signal intensity reduces the Stark splitting and can, depending on the sign of the detuning, turn the coupling either up or down.

The χ coefficients defined above [cf. Eq. (29)] can be used to develop a feeling for the way in which the two zero-frequency amplitude quadratures interact. Each amplitude quadrature can be expressed in terms of the other amplitude quadrature and the appropriate atomic and input noise by the linear estimators

$$X_s = -\frac{\chi_{sp}}{\chi_{ss}}X_p - \frac{1}{\chi_{ss}}(X_s^a - \sqrt{2/\kappa_s}X_s^{\mathrm{in}}),$$

(37a)

$$X_p = -\frac{\chi_{ps}}{\chi_{pp}}X_s - \frac{1}{\chi_{pp}}(X_p^a - \sqrt{2/\kappa_p}X_p^{\text{in}}). \qquad (37b)$$

By either substituting the series results given above in Eq. (30) or using the plots given in Fig. 5, considering probe tunings to either side of the Rabi level and assuming that atomic noise levels remain moderate, we see the following.

(i) $\nu < 0$. A fluctuation in X_s triggers a change of equal sign in X_p and a fluctuation in X_p triggers a change of opposite sign in X_s. Thus any increase in X_s causes a proportional increase in X_p, which acts back on X_s as a restoring force. This is the essence of damping and will cause a smoothing out of amplitude fluctuations in the signal field.

(ii) $\nu > 0$. A fluctuation in X_s triggers a change of opposite sign in X_p and a fluctuation in X_p triggers a change of opposite sign in X_s. Thus a fluctuation in X_s will act back on itself to cause enhancement so that the system will become unstable.

Such effects were not present in the squeezer model where the absence of a cavity for the probe did not allow for the buildup of appreciable mode cross correlation. It is clear that, regardless of the sign of ν, slow signal fluctuations can imprint themselves on the probe amplitude. While these considerations demonstrate clearly why squeezing is possible in this model, they do not reveal the physical mechanism responsible. To accomplish this we will take advantage of the formal similarity of a zero-frequency fluctuation analysis and an adiabatic analysis. A zero-frequency analysis only applies to slow field fluctuations, which the atoms will follow adiabatically.

From Eq. (35a) above, we can see that

$$\sigma_{12} \approx -i\frac{\Omega_s^*\sigma_{13}}{\Delta}. \qquad (38)$$

Since the two-photon coherence is of the order of unity and $|\Omega_s| \gg 1$, this implies that the dominant form of absorption and emission on the probed transition is via three-photon processes involving one probe and two signal photons. This is expected since the probe is far from resonance, causing single photon events to be scarce. For the signal mode, the situation is different, with the atomic coherence σ_{23} able to be expressed as the difference of two terms of comparable size as illustrated by Eqs. (35b) and (36).

If we examine χ_s [cf. Eq. (29a)], we see that the imaginary part is entirely determined by the two-photon coherence, but the real part, which determines the dissipative behavior of the atoms, has contributions from both terms. It can be shown that the population difference makes a somewhat larger contribution and thus determines the weak atomic response to the signal beam.

An in-depth analysis reveals that the net contribution from the population difference is due to the small fraction of population in $|3\rangle$ that spontaneously decays to level $|2\rangle$ (cf. also Sec. II). We may write

$$\sigma_{23} = \frac{-\Omega_s}{\gamma_1 + \gamma_2}\left(\frac{\gamma_2(\gamma_1 + \gamma_2)}{I_s}\sigma_{33} + i\text{Im}(\Omega_p^*\Omega_s^*\sigma_{13}/I_s)\right). \qquad (39)$$

The upper signal level is mainly populated by stimulated two-photon absorption from the ground state. In the steady state there will be an equal number of time-reversed processes due to their coherent nature, so that net loss for the signal can only occur through single-photon absorption after a spontaneous decay from $|3\rangle$.

We can now use our results to explain the general physical mechanism responsible for signal amplitude noise reduction. Let us first discuss the situation for positive ν, the regime of good squeezing in the single mode squeezer model.

The inclusion of a cavity for the probe means that probe fluctuations, having built up as a result of signal fluctuations, can act back on the signal to induce fluctuations in the populations of the signal transition levels. At first sight this may seem like an argument in time, which would not be appropriate for the zero-frequency component of the variance. However, the zero-frequency argument is equivalent to the time argument provided the atoms relax much faster than the fields [19]. The relative sizes of the χ_{kl} coefficients (cf. Fig. 5) shows that X_p will follow X_s adiabatically, with the probe responding almost instantaneously to signal fluctuations.

$\nu > 0$. Suppose a slow fluctuation increases the amplitude of the signal. This will alter the effective detuning of the probe due to the intensity dependence of the ac Stark effect, moving the probe closer to resonance with the lower Rabi level and increasing the coupling. Absorption from the probe field increases due to an enhancement of lossy Raman transitions between levels 1 and 3. The population in the two levels of the signal transition depends crucially on the strength of the probe field, as can be seen from

$$\sigma_{33} + \sigma_{22} \approx 2\sigma_{33} \approx \frac{2\Gamma I_p}{I_p(3\Gamma + \gamma_1) + \gamma_1(\Gamma^2 + 4\nu^2)}. \qquad (40)$$

A weaker probe will inevitably result in less population in the excited state. Thus the basic principle of noise reduction at work in the squeezer setup will be undermined since the probe light is damped faster and more efficiently than the signal light can relax.

A decrease in X_p will always create an environment fostering the signal amplitude regardless of the sign of ν, as can be seen from Eq. (37b). Depending on the size of C_p and ν, a substantial increase in signal fluctuations can occur due to less attenuation.

$\nu < 0$. In this tuning limit an increase in the signal will turn down the probe-atom coupling and thus reduce the absorption of probe photons. The subsequent increase in probe intensity now feeds back into the signal as additional damping by means of an increase of excited-state population. This will suppress signal amplitude fluctuations. The reason is that the increased intensity of the probe competes with the reduced coupling strength to actually increase the population in the intermediate level

for certain sets of parameters. This increased population can then absorb more photons from the signal, damping out the fluctuations.

Note that the above suffices to explain the general noise reduction mechanism at work and has its merits in providing us with a simple picture. It does not, however, account for all the details of the interplay of the two modes. In particular, it needs to be mentioned that, for certain negative ν, the probe amplitude only follows the signal amplitude adiabatically in an approximate sense.

For probe detunings for which the quantum-noise reduction mechanism works best the eigenvalues λ_j of the matrix χ_{gh} [formed by the four coefficients given in Eqs. (30)] develop a nonvanishing imaginary part. Assuming for the sake of simplicity that both cavity decay rates are equal to a value κ and defining

$$\lambda_j = \tfrac{1}{2}\mathrm{Tr}(\chi_{gh}) \pm \left[\tfrac{1}{4}\mathrm{Tr}(\chi_{gh})^2 - \det\chi_{gh}\right]^{1/2}, \qquad (41)$$

we find that $-\omega_c^2 = \tfrac{1}{4}\mathrm{Tr}(\chi_{gh})^2 - \det\chi_{gh} < 0$ (in units of κ). As a result no genuine adiabaticity is present in the interaction. However, if we average the fluctuations over times larger than $1/\omega_c$ we will again find that the two modes evolve in unison.

In Fig. 7(a) we contrast the predictions for the spectral variance $\mathrm{V}(X_{s,\omega}^{\mathrm{out}})$ of the signal output amplitude for Λ and ladder-configuration atoms, plotting the spectral variance of the signal amplitude for the same parameters as in Fig. 5 and for $\nu = -1$. It appears that the performance of ladder atoms is superior to that of Λ atoms for substantially nonzero frequencies. Note that for Λ atoms the spectrum displays a hump centered around $\omega = \omega_c \approx 1.38\kappa$. This thus leads to a narrowing of the frequency range for which we can expect efficient noise suppression. In Fig. 7(b) we again plot a comparison between the two configurations, in the clearly adiabatic limit of $\kappa/\gamma_1 = 0.1$. The dotted line serves the purpose
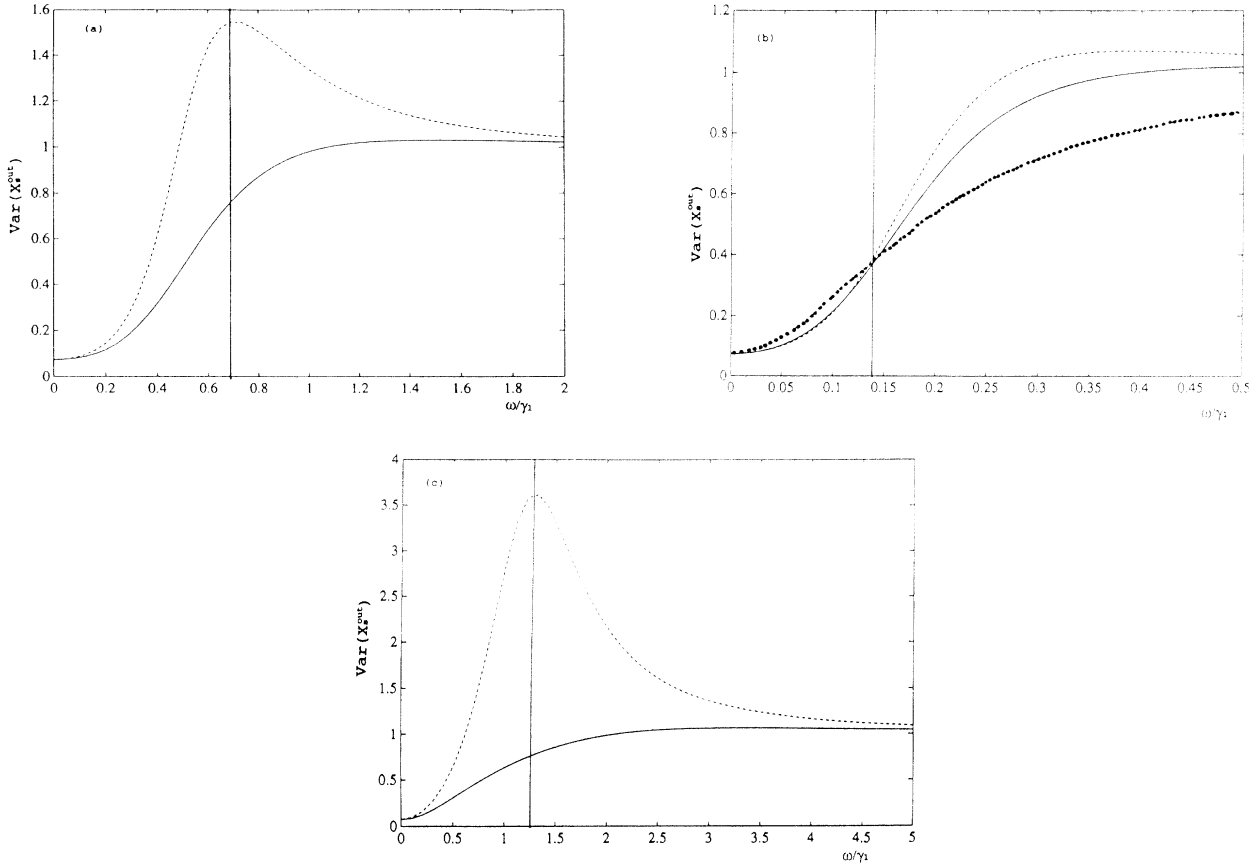
FIG. 7. (a) Spectral variance of the output signal amplitude for the same parameters as in Fig. 5 and $\nu = -1$. The continuous line is for ladder atoms, while the dashed line is for Λ atoms for the same parameters. Note that substantial noise reduction is only present for frequencies $\omega \ll \omega_c \approx 1.38\kappa_s$, which is denoted by the vertical lines. The most surprising feature is that, for ladder atoms, the excess noise centered on ω_c is completely absent. Our numerical investigations suggest that the signal coherences, all else being equal, will decay faster in the ladder system, thus preserving the adiabaticity for faster cavities. (b) The adiabatic limit. All parameters are the same as in (a), except for $\kappa_s = \kappa_p = 0.1$. The continuous and dashed lines are the same as in (a) while the dotted line, representing $1 - [1 - \mathrm{V}(X_s^{\mathrm{out},0})]4\kappa^2/(4\kappa^2 + \omega^2)$, is a close approximation to the *squeezer* spectrum for the same parameters. Note that the noisy hump has become far less prominent for the Λ system. (c) The case of strongly damped cavities with the dashed line as above. We set $\kappa_s = \kappa_p = 4\gamma_1$ and leave all other parameters as in (a). Again the excess noise at ω_c is absent for the ladder configuration. Because the noise suppression mechanism depends on spontaneous emission, only a band of frequencies satisfying $\omega \lesssim \gamma_1$ exhibit squeezing.

of illustrating the narrowing effect of an oscillatory behavior of the fluctuations. Its functional dependence on ω is given by $1 - [1 - V(X_s^{out,0})]4\kappa^2/(4\kappa^2 + \omega^2)$, which is of the same form as the result obtained for the squeezer model [20]. For frequencies larger than 1.38κ this curve no longer gives a satisfactory fit. Switching to the nonadiabatic limit of strongly damped cavities, we find that noise suppression is limited by the rate at which the atomic system can relax, which thus defines the relevant internal time scale. The bandwidth of the squeezing is now limited by the size of the spontaneous decay rates, as illustrated in Fig. 7(c).

The squeezing in the two-mode ghost transition model is another example of the utility of atomic coherence. Clearly, the range of probe detuning for which squeezing persists has been narrowed in comparison with the squeezer. An extension of this range could be achieved by exploiting the correlation between the output light from the probe and the signal cavities. A measurement performed on the probe output light can be used to correct some of the fluctuations still present in the signal output light. It has previously been shown that conditioning the signal output on a measurement of the probe output can lead to substantial further improvement in the squeezing for Λ atoms [8]. The feasibility of such an undertaking has already been demonstrated in a quantum feedforward scheme using twin beams from an optical parametric oscillator [21].

VII. CONCLUSIONS

We have shown that dressed three-level atoms can be used to generate significant squeezing in the amplitude of a strong signal field even if the signal is resonant with a bare atomic transition. We have considered the interaction of three-level atoms in the ladder configuration with a strong cavity field applied to the upper transition and a weak probe field to the lower transition. The weak field is tuned close to resonance with one of the Rabi levels created by the driving of the atoms with the strong signal field.

In the first configuration considered the probe light is applied in transmission. Noise reduction can be achieved for tuning the probe close to the outside of the Autler-Townes doublet. As the mechanism responsible we have identified the sensitivity of the excited-state population to the size of the detuning between the probe light and the Rabi level, which in turn depends on the strength of the cavity field. This can be exploited to stabilize the intensity of the cavity field and reduce the fluctuations in the amplitude of the output light below the shot-noise limit.

In the ghost transition scheme we have found that quantum-noise reduction can be achieved with both probe and signal being allowed to resonate in a cavity. Although there are similarities between the two configurations, the physical mechanism responsible for the squeezing is totally different. For the tuning limit in which the squeezer works best we now encounter unstable behavior because of detrimental positive feedback from the probe fluctuations whereas tuning to the inside of the Autler-Townes doublet causes negative feedback, which provides a damping mechanism for the signal amplitude fluctuations.

The size of the field dressing the upper atomic transition ensures that absorption from the mean field is small. The strong field thus creates a self-induced transparency in the atomic medium. Nonlinear absorption used to suppress intensity fluctuations is nevertheless greatly enhanced. The combination of small losses from the coherent input field into the cavity in conjunction with the convincing amount of noise reduction raises hopes that atomic coherence will play a role in efforts to find an efficient scheme for the conversion of coherent input light into bright-squeezed output light.

ACKNOWLEDGMENTS

[1] J. Opt. Soc. Am. B **4**(10) (1987); special issue on Squeezed States of the Electromagnetic Field, edited by H.J. Kimble and D.F. Walls; Appl. Phys. **B55**(3) (1992), special issue on Quantum Noise Reduction in Optical Systems—Experiments, edited by E. Giacobino and C. Fabre.

[2] R. E. Slusher, L. W. Hollberg, B. Yurke, J. C. Mertz, and J. F. Valley, Phys. Rev. Lett. **55**, 2409 (1985).

[3] S. E. Harris, Phys. Rev. Lett. **63**, 1033 (1989); S. E. Harris, J. E. Field, and A. Imamoğlu, ibid. **64**, 1107 (1990); A. Imamoğlu, J. E. Field and S. E. Harris, ibid. **66**, 1154 (1991).

[4] M. O. Scully, Phys. Rev. Lett. **67**, 1855 (1991).

[5] K. Hakuta, L. Marmet, and B. P. Stoicheff, Phys. Rev.

Lett. **66**, 596 (1991); Phys. Rev. A **45**, 5152 (1992).

[6] K.-J. Boller, A. Imamoğlu, and S. E. Harris, Phys. Rev. Lett. **66**, 2593 (1991); J. E. Field, K. H. Hahn, and S. E. Harris, ibid. **67**, 3062 (1991).

[7] Klaus M. Gheri and Daniel F. Walls, Phys. Rev. A **46**, R6793 (1992).

[8] K. M. Gheri and D. F. Walls, Phys. Rev. A **49**, 4134 (1994).

[9] J.-Ph. Poizat, M. J. Collett, and D. F. Walls, Phys. Rev. A **45**, 5171 (1992).

[10] K. M. Gheri, P. Grangier, J.-Ph. Poizat, and D. F. Walls, Phys. Rev. A **46**, 4276 (1992).

[11] C. W. Gardiner, Quantum Noise (Springer-Verlag, Berlin, 1991).

[12] N. G. van Kampen, *Stochastic Processes in Physics and Chemistry* (North-Holland, Amsterdam, 1992).

[13] J.-M. Courty, P. Grangier, L. Hilico, and S. Reynaud, Opt. Commun. **83**, 251 (1991).

[14] J.-M. Courty and S. Reynaud, Phys. Rev. A **46**, 2766 (1992). It is also demonstrated in this paper that a *semiclassical* susceptibility (response to a small classical modulation) is equal to the *microscopic* susceptibility (response to quantum fluctuations). We have made use of this property in our Taylor series expansion.

[15] Clearly, if the frequency of the coherent input is not resonant with the cavity mode, $d\mathbf{L}_f$ will depend on the cavity mistuning ϕ, as introduced in Eq. (2a).

[16] Two things should be noted here: (i) I_s will actually be $g^2|\alpha|^2$, but, since g is constant, this does not detract from the sense of the exposition. (ii) χ_{XX} cannot be obtained by simply using Eqs. (7b) and (12) and differentiating. Differentiation must take place before the series expansion is made, so that no confusion arises between I_s and Δ_0^2.

[17] J.-Ph. Poizat and P. Grangier, Phys. Rev. Lett. **70**, 270 (1993).

[18] Note that the two decay rates γ_1 and γ_2 are now made equal. Although this ratio gives the best noise suppression, we did not impose this condition in the analysis of the *squeezer*.

[19] Basically the same arguments hold for the diabatic limit of strongly damped cavities, $\kappa > \gamma$, provided we consider slow fluctuations with long autocorrelation times. The width of the spectral band for which noise reduction takes place is now limited by the atomic linewidth and not by the cavity bandwidth.

[20] For optimum squeezing we find that χ_s, which defines the width of the spectrum, will attain a value $2\kappa_s$.

[21] A. Heidmann, R. J. Horowicz, S. Reynaud, E. Giacobino, C. Fabre, and G. Camy, Phys. Rev. Lett. **59**, 2555 (1987); T. Debuisschert, S. Reynaud, A. Heidmann, E. Giacobino, and C. Fabre, Quantum Opt. **1**, 3 (1989); J. Mertz, T. Debuisschert, A. Heidmann, C. Fabre, and E. Giacobino, Opt. Lett. **16**, 1234 (1991).